Formation of residual stresses in austenitic stainless steels by infeed and recess rotary swaging

Holger Hoche[1], Fabian Jaeger[1], Alessandro Franceschi[2], Matthias Oechsner[1], Peter Groche[2]

[1] Technische Universität Darmstadt, Center for Structural Materials MPA-IfW, Grafenstr. 2, 6283 Darmstadt, Germany

[2] Technische Universität Darmstadt, Institute for Production Engineering and Forming Machines, Otto-Berndt-Straße 2, 64287 Darmstadt, Germany

Corresponding author: hoche@mpa-ifw.tu-darmstadt.de

Keywords: 1.4404, 1.4307, austenitic stainless steel, residual stresses, rotary swaging, X-ray diffraction, sin² Ψ

Abstract

The austenitic stainless steels 1.4307 and 1.4404 significantly benefit from cold forming, due to their high work hardening capability. Great potential to improve the component's fatigue properties is expected by optimizing the forming process chain such that specific residual stresses are induced in critical component areas. In this work, an analysis of the formation of residual stresses during rotary swaging is carried out. Through this incremental forming process, high strain hardening and a complex material flow history are induced in the workpieces. Therefore, measuring strategies for the residual stress measurement of cold deformed austenitic steels by X-Ray diffraction, using the $\sin^2\Psi$-method, were developed. Here, especially the 1.4307 is a challenging material due to cold forming induced martensite formation. Despite phase changes, both cold formed materials exhibit anisotropic microstructures as well as coarse grained areas. Moreover, particular notched geometries are produced on the workpieces by rotary swaging. The measuring techniques are further developed for these complex geometries and the residual stresses are investigated.

Introduction

Rotary swaging is a well-established forming technology in the automotive and aerospace manufacturing industries for the forming of axial symmetric bars and tubes [1]. According to the German standard DIN 8583 it belongs to the open die forming processes [2]. The advantages of this incremental process lie in particular in its high flexibility combined with low investment and tooling cost, due to the relatively low forming forces needed [3]. Moreover, rotary swaging offers some important advantages on the product side. Very hard materials can be worked and the final parts exhibit high static and cyclic strength due to strain hardening [4]. Two main process variations can be distinguished: the infeed and the recess rotary swaging. These variants differ for the direction of the feed motion, as schematically represented in Figure 1. The infeed rotary swaging process feeds, the workpiece with an axial motion into the machine. The working tools oscillate radially and reduce the diameter of the workpiece along the whole feed length. By recess rotary swaging, the workpiece has no axial motion. In this process, the forming is performed by the radial movement of the working tools, which is superposed to their oscillation. In this way, a localized reduction of the workpiece occurs according to the tool geometry. Infeed and recess rotary swaging can also be combined to obtain geometries that are more complex.

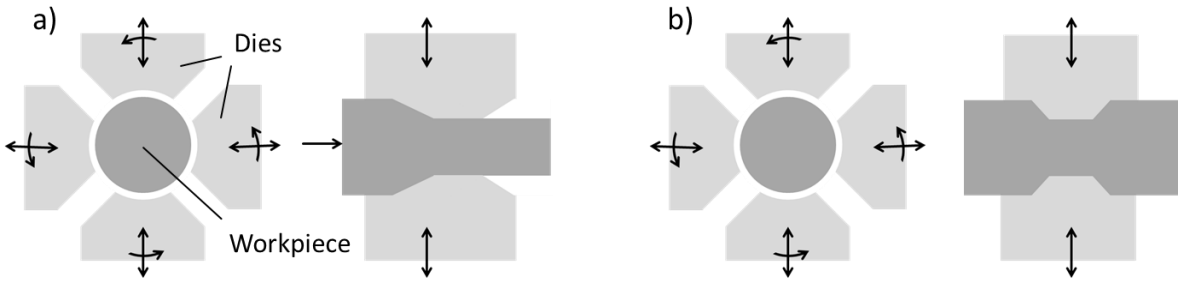

Figure 1: Schematic representation of infeed (a) and recess (b) rotary swaging

Decisive product qualities for cold formed components are the residual stresses, especially in the near-surface area. However, in the literature, incremental processes are not analysed to the same extent as conventional continuous

technologies. Investigations of residual stresses in rotary swaged products are mainly related to the forming of tubes [1, 5].

The researched materials are the austenitic stainless steels 1.4404 (X2CrNiMo17-12-2, AISI 316L) and 1.4307 (X2CrNi18-9, AISI 304L). Due to their high chrome and nickel content, the materials exhibit good resistance against both oxidation and electrochemical corrosion [6]. Stainless austenitic steels have a great flow behaviour, which makes them extremely suitable for cold working processes [7]. The high deformability is coupled with strain hardening during the deformation, leading to localized enhanced mechanical properties. The challenge with strain hardening is the formation of residual stresses, which have not been extensively researched yet. Especially the targeted employment of compressive stresses by cold forming could be beneficial for the component lifetime and safety. Both 1.4404 and 1.4307 are used in the food industry due to their great corrosion resistance.

There exist several challenging factors when performing residual stress measurements of austenitic stainless steels. Due to the cold forming process, they reveal a texture, which depends on the local degree of deformation. Moreover, coarse grains make it difficult to measure a sufficient number of grains to achieve results with good statistics. The texture complicates the measurement further, since it leads to a shift of the reflex width based on orientation as well as the interference lines. Therefore, $d(\sin^2\psi)$ plots are not linear, if the sample is textured [8], making the analysis more elaborate. Another challenge is the sample geometry. Since rotary swaging usually produces cylindrical work pieces, there are not flat surfaces, where X-ray diffractometry can be performed easily. Additionally, recess rotary swaging forms notches, which are difficult to examine due to shadowing effects.

The present paper investigates the formation of residual stresses in rotary swaged parts of the materials 1.4307 and 1.4404. Measurements of residual stresses in these rotary swaged parts are challenging due to local non isotropic strain hardening and texture formation. Especially the 1.4307 makes the matter more complex due to cold forming induced martensite formation. Moreover, the literature provides sparely information about the stress state of rotary swaged components. The task is to provide a better description of the residual stress generation in rotary swaged parts.

Materials and methods

Samples of the materials 1.4307 (0.024 C, 0.275 Si, 2.01 Mn, 0.033 P, 0.034 S, 18.16 Cr, 0.295 Mo 8.00 Ni, 0.07 N) and 1.4404 (0.022 C, 0.413 Si, 1.35 Mn, 0.031 P, 0.027 S, 17.72 Cr, 2.01 Mo, 9.90 Ni, 0.04 N) were milled from billets belonging to the same batch of raw material, to ensure identical material properties. Cylinders, respectively 14.5mm and 10.78mm in diameter, were realized for infeed and recess rotary swaging. These parts were then solution annealed in a preheated vacuum oven for 15 minutes at 1050°C and cooled in air. Prior to the cold deformation, a lubricant was applied on the samples surfaces. The parameters used for infeed and recess rotary swaging are summarized in Table 1.

Table 1: Parameters used during the rotary swaging

Parameter	Infeed rotary swaging	Recess rotary swaging
Rotational speed [rot/min]	50	
Feeding velocity [mm/min]	100	-
Hub [mm]	0.7	
Frequency of hub [Hz]	29	
Radial velocity [mm/min]	-	50
Final diameter [mm]	10.9	10.38

In Figure 2, the tools used for the experiments are shown. For infeed rotary swaging, the diameter of the workpiece is reduced with an entry angle of 4°. The length of the forming and calibrating zones are 50mm each. With the second tool (Figure 2b), two different notched geometries can be manufactured on the samples through recess rotary swaging. The radii of these notches are 1.25 and 2.5mm, respectively.

The residual stresses were determined by X-ray diffraction (XRD) according to DIN EN 15305 using the $\sin^2\Psi$-method. Therefore, a diffractometer made by Stresstech, model XStress G3R in a modified Ψ-arrangement was used. The residual stresses were calculated from 7 equidistant Ψ angles from 0° to + 45° and from 0° to − 45°, respectively. Mn Kα radiation was used for the measurement of the austenitic residual stresses since it yields better results for austenitic steels than Cr Kα. With Mn Kα radiation the reflex (311) can be measured which exhibits double the multiplicity of the (220) reflex, which is measured with Cr Kα radiation [8]. The measurements in the

martensitic phase as well as the determination of the martensite content were performed with Cr Kα raditation. The cylindrical samples produced by the rotary swaging process have a diameter of approx. 1 cm. Since the maximum aperture for this kind of measurement should not exceed a tenth of the diameter of curvature of the sample, acc. to DIN EN 15305, the aperture was set to a diameter of 1mm. The X-ray elastic constant used to calculate the residual stress values was ½S2 {311} = 7.57 × 10^{-6} mm^2/N for austenite and ½S2 {211} = 5.82 × 10^{-6} mm^2/N for martensite [9].

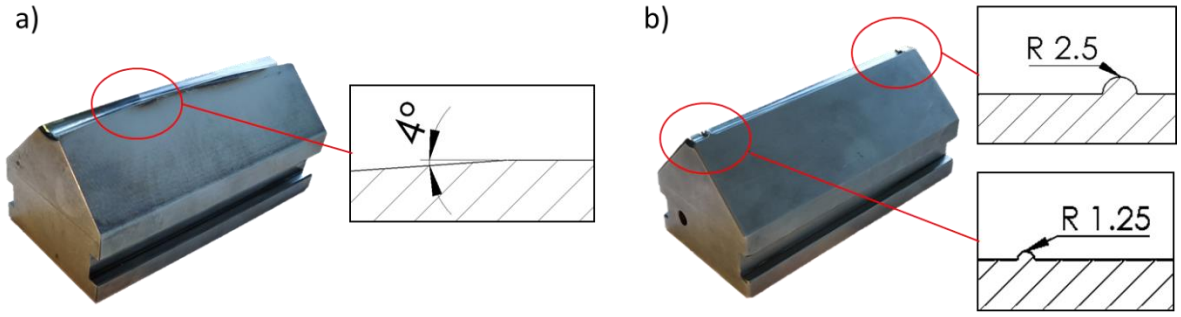

Figure 2: Forming tools used for infeed (a) and recess (b) rotary swaging

To measure residual stress depth profiles of the material 1.4404, an electro-polishing machine type Struers Movipol-3 was employed. The polishing process was stopped at 0.125, 0.25, 0.5 and 1.0 mm to perform residual stress measurements.

In addition, microspecimens were prepared and examined by optical microscopy to reveal the influence of the rotary swaging process on the materials microstructures. Also microhardness depth profiles were conducted at the micro-specimens. In addition, hardness measurements were also performed on the surfaces of the specimens.

Results

The analysis of the initial state of the samples was already performed in [7]. After the solution annealing of the machined samples, the metallographic examinations of both materials showed a purely austenitic microstructure without deformation-induced defects. With a Vickers hardness of 151.4 HV 0.3 for 1.4307 and 143.3 HV 0.3 for 1.4404, the hardness values are in the characteristic range of solution annealed microstructures of the respective materials. Significant differences between the two materials were observed in the grain sizes. The grain size of 1.4307 was determined to G =4, which according to Table C1 of DIN EN ISO 643 corresponds to an average of about 128 grains/mm^2. With a grain size of G =5.5, the microstructure of 1.4404 is significantly finer, revealing an average of 384 grains/mm^2. The X-Ray measurements showed for both materials these samples are close to a residual stress-free state.

The residual stresses on the samples manufactured through infeed rotary swaging were analysed along the path shown in Figure 3. Along this path, three regions can be distinguished:

- The section I goes from 0 to 50mm. Here the sample has been fully deformed and calibrated by the working tools.
- In section II, from 50 to 100mm, the sample has been reduced to its final geometry, but it is still inside the calibration zone at the end of the process
- From 100 to 120mm the sample is still in the forming zone and has not reached its final diameter, which can be inferred from its curvature.

Measurements through X-Ray diffraction were performed both in axial and tangential direction on the components' surface. The results of the surface residual stresses measurements after the infeed rotary swaging are displayed in Figure 5.

In all the measured points, these samples are characterized by compressive residual stresses on the surface. In general, the quality of the $\sin^2\Psi$ -plots is very good and complies with the criteria to assess the measurement quality of cold deformed parts in [7]. The axial compressive stresses are both, in section I and II, significantly higher than the tangential stresses. In particular in section I, the axial as well as the tangential stresses of both materials are in good compliance with each other, showing a quite constant behaviour. This means that the calibration process had the desired effect of producing a defined residual stress state. Some differences can be observed between the behaviour

of the axial and tangential stresses in the second section. In the axial direction, the compressive residual stresses tend to increase along the formed section. In the tangential direction instead, the residual stresses fluctuate stronger than in section I, but there is no definite trend identifiable. In section II, the axial compressive residual stresses of 1.4404 exhibit higher values than 1.4307, which is interesting it signifies a change to the behaviour in section I. Nevertheless, the measured residual stresses of sections I and II do not show significant differences which could be correlated with the material microstructure, in particular the martensite formation in 1.4307. In section III the size of the fluctuations in residual stresses is very pronounced in 1.4404 for the tangential stresses. At the beginning of section III there is a sudden increase of the compressive residual stresses in comparison with the previous section. The material 1.4307, on the other hand, does not show this effect. The martensite content of 1.4307 can be seen in Figure 4. In section I it is higher the closer the measured point is to the tip of the sample. Between the middle of section I and the middle of section II the martensite content does not change. At the end of section II the martensite content is zero. However, in section III the martensite content is again relevant. The martensite content of 1.4404 was measured as well, but was under the detection limit.

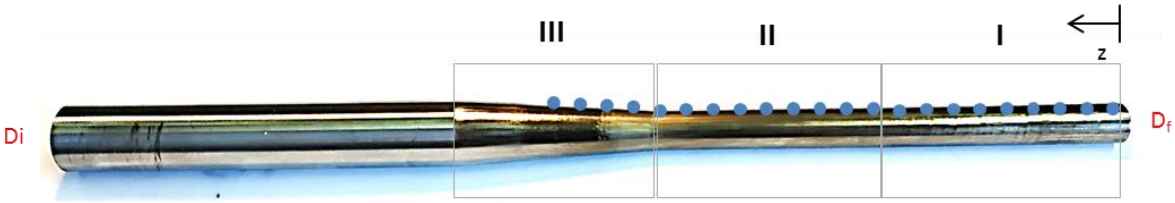

Figure 3: Position of the measurements of the residual stresses through X-Rays on the samples produced by infeed rotary swaging

In section I the hardness exhibits the highest values for 1.4307 due to the highest degree of deformation achieved by forming as well as calibration. This correlates with the evolution of the compressive residual stresses, which exhibit higher values in section I due to the calibration process. Additionally, 1.4307 exhibits higher hardness values than 1.4404, which could be an effect caused by martensite formation. In section II the hardness of 1.4307 slightly drops. The decrease in hardness of 1.4307 is approx. 50 HV 0.1. In section III the surface hardness of 1.4307 increases again, which could be an effect of the high degree of cold deformation even in this section. The hardness of 1.4404, however, is homogeneous over the length of the sample. The higher hardness of 1.4307 can be explained with the formation of deformation martensite. The reason for the deviating hardness values appears to be, that the different points of this section have undergone different stages of calibration.

For the material 1.4404 the tangential residual stresses are nearly identical in section I and II and only slightly differ in section III. For material 1.4307 instead, there is a sudden decrease of the austenitic compressive residual stresses in comparison with the previous section. In section III the data shows even bigger fluctuations which could be due to inhomogeneous deformation in the section. In the martensitic phase the axial stresses are bigger than the tangential ones, mirroring the austenitic behaviour. The martensitic compressive stresses are higher than the austenitic ones. Since the forming of martensite is caused by deformations it is plausible that zones with higher deformation would both have greater stresses and more martensite formation.The relatively low stresses at 905 and 100 mm are measurement artifacts caused by the low martensite content in those points leading to bad signal to noise ratio.

In Figure 6 the different microstructures in the infeed rotary swaged samples are exemplarily shown for sections I and III. In comparison to the annealed state, the grains are refined by the rotary swaging process. Unfortunately, due to the texture, the grain size according to DIN EN 643-1 cannot be assessed. In general, the microstructure of 1.4404 is finer that of 1.4307, which also corresponds to the differences in grain sizes in the solution annealed state. In both, section I and III, the microstructures are uniform up to a depth of approx. 4 mm from the surface. 1.4404 exhibits deformation structures like slip bands, which are more pronounced in section I due to the higher degree of cold deformation. The microstructure of 1.4307 also indicated the formation of deformation induced martensite, which could be proved by a noticeable magnetism of this material. In the case of 1.4404, the magnetism is negligible.

Figure 7 shows an axial cross section of section III of 1.4404. It is visible that the surface of the sample has cracked, which released residual stresses. Processes like this are one of the reasons for the unsteadiness of residual stress measurements.

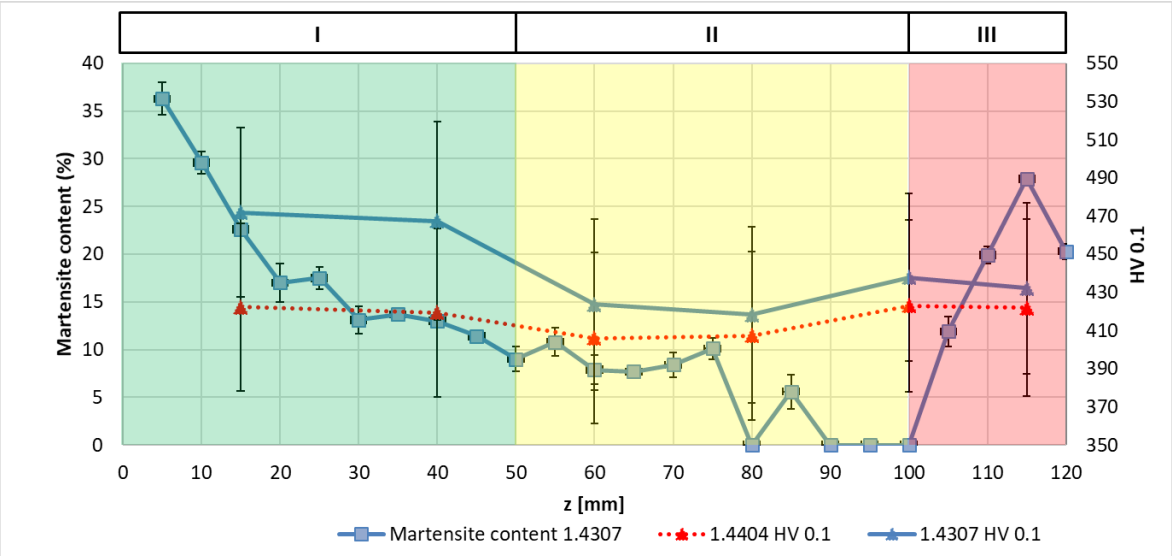

Figure 4: Martensite content of 1.4307 and result of the hardness measurements on the samples manufactured through infeed rotary swaging. The Martensite content of 1.4404 was measured as well, but was not present in a detectable quantity. For this reason it is not reported in the diagram.

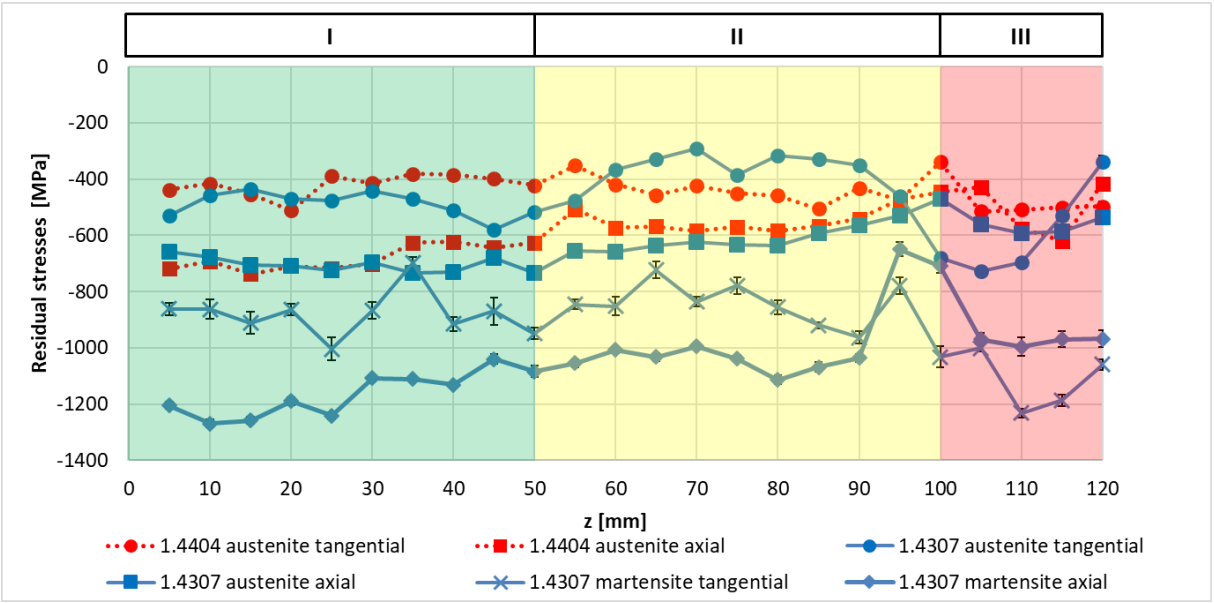

Figure 5: X-Ray residual stresses measurements on the samples manufactured through infeed rotary swaging. The martensite phases of 1.4404 was not measured, since the percventage of it is below the detection limit.

Through recess rotary swaging, notches with radius 1.25 and 2.5 mm, respectively, were produced on the solution-annealed samples. A distance of 15mm was maintained among the notches to avoid mutual influence on the stress state. The process was performed with the parameters shown in Table 1. After reaching the final radial position, the tools were kept oscillating in position for two seconds for calibrating the samples. Then the residual stresses were measured on the bottom of each cavity in eight different points. In Figure 8, the positon of these X-Ray measurements along the circumference of the samples is clarified.

Figure 9 shows the residual stresses measured on both 1.4307 and 1.4044 in the 1.25 mm and 2.5 mm notches for the austenitic (left) and martensitic (middle) phases as well as the martensite content (right). Although the notches complicate the measurements, there are only small errors and the criteria of [7] are fulfilled. Although the measurements scatter within the 6 measurements in the 90° Section, some trends are still identifiable. In the 2.5 mm notches of 1.4307 the highest axial austenitic compressive stresses can be observed. Depending on the angle, the stress values fluctuate between -260 MPa and -500 MPa without any dependency on their circumferential position. The compressive stresses inside the 1.25 mm notch of 1.4307 are systematically on a lower level and vary from -160 MPa at 0° to -250 MPa. Only at the 90° position, a value of only -60 MPa was measured which may be caused by microstructural artefacts, e.g. by material overlapping.

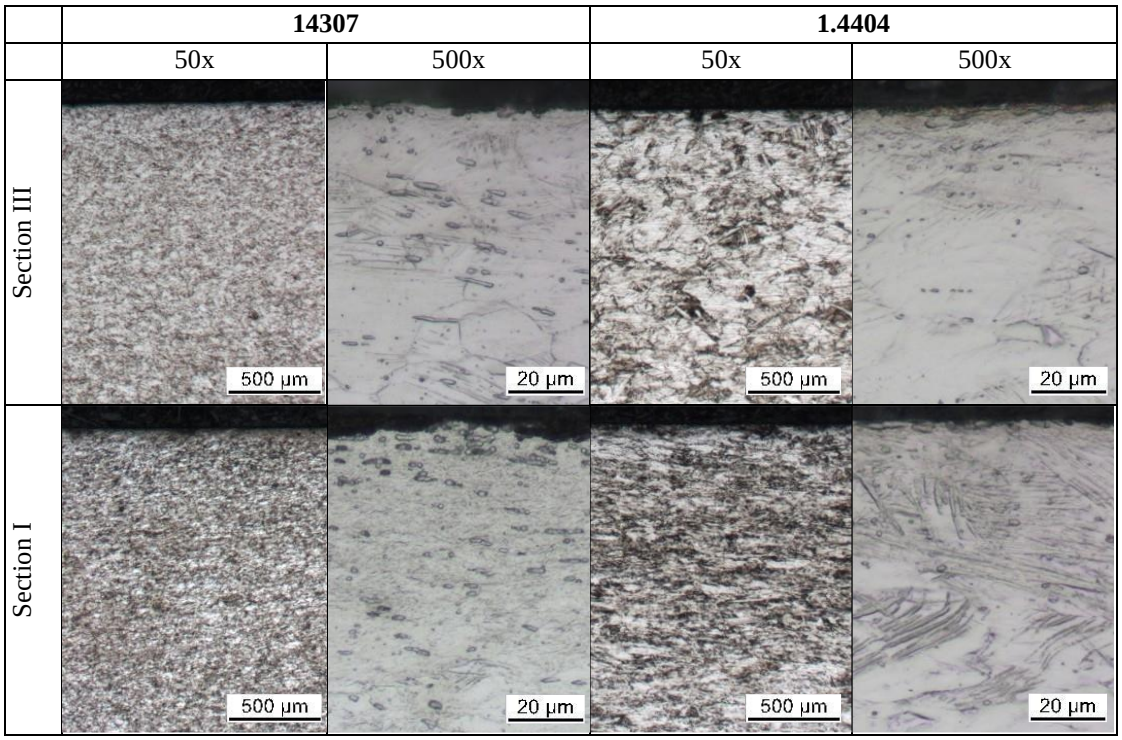

Figure 6: Microstructure analysis by optical microscopy of sections I and III, V2A-etchant. The initial micrographs can be seen in [7].

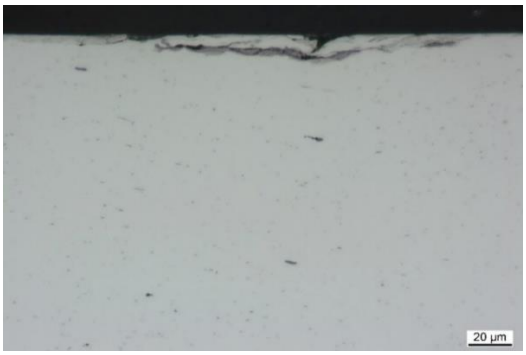

Figure 7: Exemplary figure of a material overlap due to rotary swaging. 1.4404, section III, unetched

The axial stresses in the 2.5 mm notch of 1.4404 exhibit a graded increase from -240 MPa at 0° to -530 MPa at 90°. While the residual stresses for the materials 1.4404 and 1.4307 show a quite good agreement for the 2.5 mm notch, the behaviour of the 1.25 mm notch is different. Unlike the 1.4307 sample, the 1.25 mm notch of 1.4404 reveals considerably higher compressive stresses with values between -190 MPa and -450 MPa. In general, it can be stated, that the axial stress values for the 2.5 mm notches fluctuate more than for the 1.25 mm ones.

In general, the tangential residual stresses comply with the axial stresses. The compliance is more pronounced for the 1.25 mm notch, while the scatter of the values is again significantly higher for the 2.5 mm notch. In particular, the 2.5 mm notch of 1.4404 has the most notable scatter in residual stresses. For all orientations and materials, the largest compressive stress is bigger for the notch produced with the 2.5 mm tool. The reason for this is the higher deformed area when using a bigger tool, which results in a greater degree of deformation. This is concurrent with the results of the samples produced through infeed rotary swaging, where the stresses were highest in the zone with the most deformation as well (see Figure 5).

The stresses of the martensitic phases show greater compressive stresses and a bigger isotropic effect. For the 1.4404 sample the axial stresses of the 2.5 mm notch (between -500 and -830 MPa) and the 1.25 notch (between -470 and -660 MPa) are bigger than the tangential stresses, which range from -380 to -630 MPa and from -270 to -520 MPa respectively. The 1.4307 sample exhibits a larger difference between the notches. In the 2.5 mm notch the axial stresses from -280 to -780 MPa are generally larger than the tangential ones from -390 to -680 MPa. This behaviour is reversed in the 1.25 notch with smaller stresses in the axial direction from -170 to -460 MPa compared to tangential stresses from -390 to -530 MPa. However, all martensitic graphs fluctuate stronger than the austenitic ones. This

can be explained by the stronger deformation processes in the martensitic phases leading to a bigger spread in compressive stresses. The martensite content itself does not change much with the position at which it is measured. It can be seen that 1.4307 is more disposed towards forming martensite than 1.4404.

Figure 8: Position of the X-Ray residual stress measurements on the samples produced by recess rotary swaging

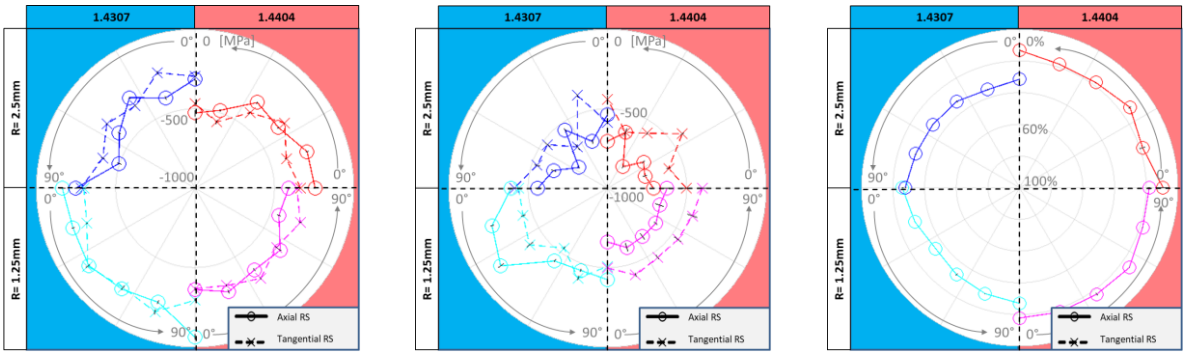

Figure 9: Residual stresses and martensite content of the notched samples. The angles are between 0 and 90° counter clockwise. The leftmost subfigure shows the residual stress in the austenitic phase, the one in the centre that in the martensitic phase and the rightmost shows the martensite content in percent.

For better understanding, Figure 10 shows the different microstructures of the notches produced by recess rotary swaging. In all of them, the notch area itself exhibits deformation structures due to strain hardening happened during the recess rotary swaging process. Here, 1.4307 and 1.4404 reveal a nearly similar degree of highly deformed microstructures. For 1.4307, there is also evidence for the presence of cold deformation induced martensite. An interesting outcome is, that the degree of deformation of the microstructure is lower for the 2.5 mm notch. The smaller 1.25 mm tool is causing a higher degree of deformation than the broader 2.5 mm tool. For the material 1.4404, this observation is in accordance with the results on the residual stress measurements. For 1.4307, the 1.25 mm notch reveals lower stresses than the less deformed 2.5 mm notch. A reason therefore could not be stated yet, but it is likely, that the formation of deformation induced martensite could change the residual stress state.

1.4307		**1.4404**	
1.25 mm	2.5 mm	1.25 mm	2.5 mm

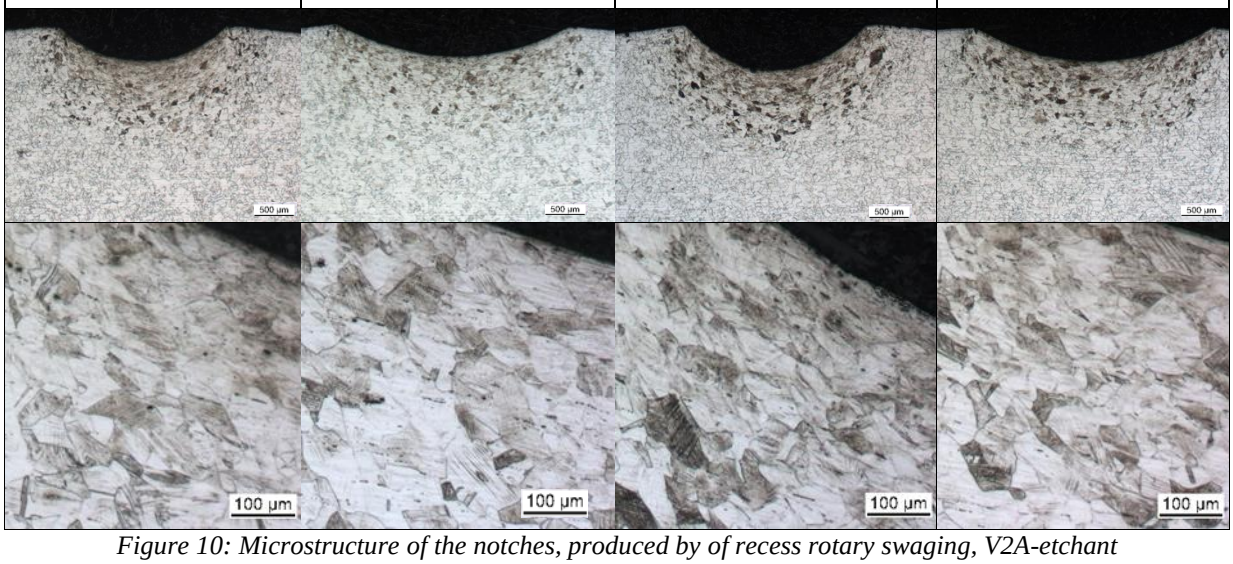

Figure 10: Microstructure of the notches, produced by of recess rotary swaging, V2A-etchant

Figure 11 shows the comparison of residual stress measurements on the same notch at angles of 0, 90, 180 and 270°, respectively. The goal is to verify the theory, that the residual stress state follows the fourfold symmetry of the tools for the recess rotary swaging. For the 2.5 mm notch in 1.4307, the residual stresses in axial as well as tangential direction are clustered between -250 and -350 MPa with the exception of a single value of -440 MPa. The residual stresses in axial direction for the 1.25 mm notch of 1.4307 are lowest in comparison to all other parameters, which complies with the circumferential measurements shown in figure 8. For the tangential direction of both notches in 1.4307, all the residual stresses are in great accordance with each other and show a low scatter. The martensitic stresses in 1.4307 are generally higher. Similar to the austenitic phase the stresses in the 1.25 mm notch are clustered closer together. For 1.4404, both, the axial and the tangential notches reveal a remarkable scatter between the angles. This is especially the case for the axial direction. The 2.5 mm notch shows values between -240 and -530 MPa and the 1.25 mm one between -190 and -450 MPa. Meanwhile, the tangential stresses are in good accordance with each other for three out of four data points, while the fourth point diverges. The martensitic stresses are higher in 1.4404 as well. The spread of the stresses is comparable to the austenitic case.

When looking at all the data points, it can be seen that the tangential stresses are generally closer to each other than the axial stresses. This is plausible, since for the recess swaged specimens, the stresses in tangential are pointing in the direction of the material flow. The same effect can be seen in Figure 5, where the material flow is in axial direction and axial stresses fluctuate less than the tangential ones. However, the theory of the existence of a fourfold symmetry of the stress state caused by the fourfold symmetry of the forming process could not be proven due to large scatter at the measured points.

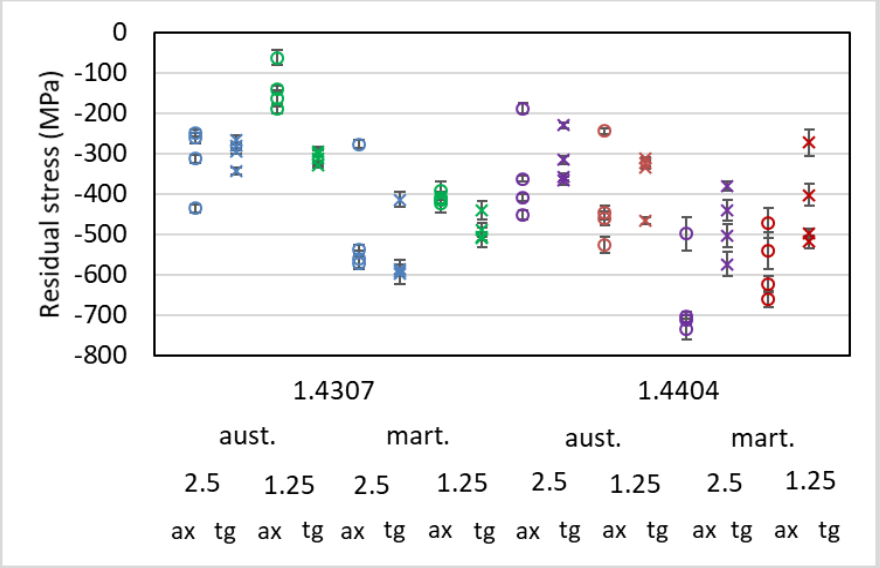

Figure 11: Comparison of residual stresses for 0, 90, 180 and 270° in all notches

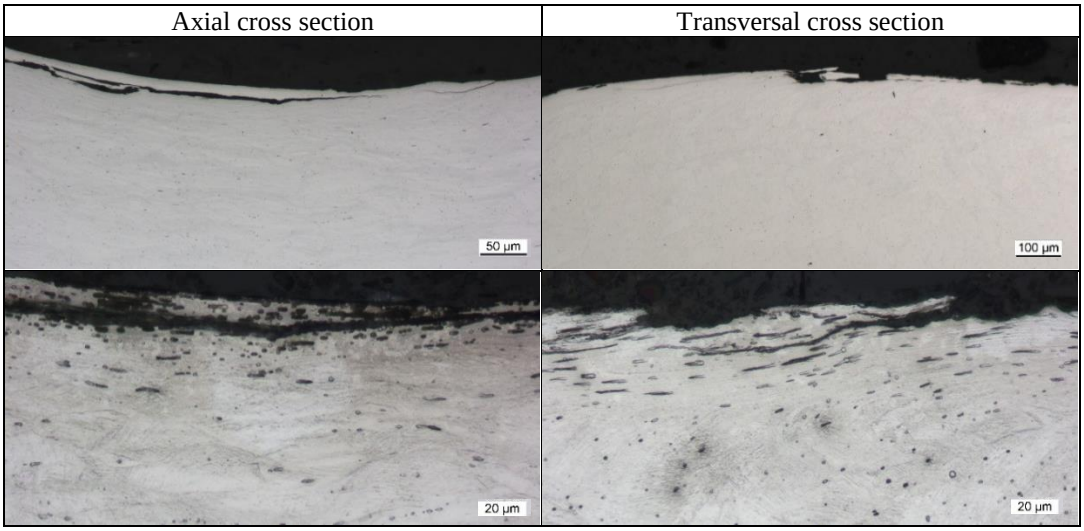

Figure 12: Microscopic pictures of the 1.25 mm notch of 1.4404 with material overlaps. The microsections are oriented axially (left hand side) as well as transversal (right hand side).

By examination of the microspecimens, some material overlaps due to the rotary swaging process are present at each specimen (Figure 12). The length of these overlaps could be up several 100 µm, while their depth is max. some 10 µm. At these sites, there is no homogenous residual stress state, since the stresses are relaxed in the overlap. The overlaps are most pronounced in the bottom of the notches, where the material flow is highest. This also complies with the XRD measurement positions. From the $\sin^2\Psi$-plot, the overlaps cannot be assessed definitely. The overlaps cause non isotropic stress states and therefore contribute to the scatter in the measurements. Moreover, these overlaps affect the cyclic properties, thus compensating the beneficial effect of the compressive residual stresses.

To further comprehend the changes going on in the material upon deformation, hardness depth profiles were recorded (Figure 13). Although an influence of the notch size on the compressive residual stresses was proven, no significant influence, neither of the notch nor the material, could be validated from the hardness depth profiles. In particular, at the surface all values scatter in a narrow range, thus indicating an identical degree of the strain hardening. With progressing depth, the hardness decreases as the effect of strain hardening lessens. Up to a depth of 0.3 mm, the hardness only slightly decreases. Even at a surface distance of more than 2.5 mm the hardness of the solution annealed state is not reached. However, 1.4404 exhibits lower values of approx. 180 HV0.1 than 1.4307 with approx. 230 HV 0.1. This coincides with the literature values of 151.4 HV 0.3 for 1.4307 and 143.3 HV 0.3 for 1.4404 in the annealed state [7]. It is of note that the decay of the hardness is roughly exponential.

This behaviour can be compared to the depth profiles of the residual stresses of 1.4404 of the 2.5 mm notch, shown in Figure 14. There, the residual stress is -200 and -390 MPa at the surface, respectively. The maximum of the compressive residual stresses is in a depth of about 0.25 mm. Exceeding this depth, both, the axial and the tangential compressive stresses decrease, where the tangential ones become tensile stresses in approx. 0.7 mm depth and the axial stresses remain compressive even at 1 mm distance from the surface. The residual stress depth profile complies with the hardness measurements, where the drop in hardness is only slightly up to 0.3 mm, which corresponds to the maximum of the compressive residual stresses.

Conclusions

The effect of infeed and recess rotary swaging techniques on the austenitic stainless steels 1.4307 and 1.4404 on the formation of the residual stresses, the changes in microstructure and the work deformation hardening was analysed. Due to rotary swaging, a grain refinement of the initially coarse grained austenitic microstructure was achieved. Both processes could induce compressive residual stresses at the surface in both, axial and tangential direction. In general, the distribution of the residual stresses exhibits less scattering in the direction of the maximum material flow, i.e. the axial direction for infeed and the tangential direction for recess rotary swaging. It was shown that rotary swaging techniques induced strain hardening and the formation of deformation structures, with both effects being more pronounced on the surface. Overall, the residual stresses comply with the degree of deformation of the microstructures. Additionally, in 1.4307 also cold deformation martensite has been formed.

Unfortunately, the rotary swaging produced several material overlaps at the surface, which could be some 100 µm in length. At these sites, the residual stresses are inhomogeneous, since the stresses are relaxed by the overlap. Therefore, these surface artefacts are likely to contribute to the scatter in the measured residual stresses. Moreover, these overlaps affect the cyclic properties, thus compensating the beneficial effect of compressive residual stresses.

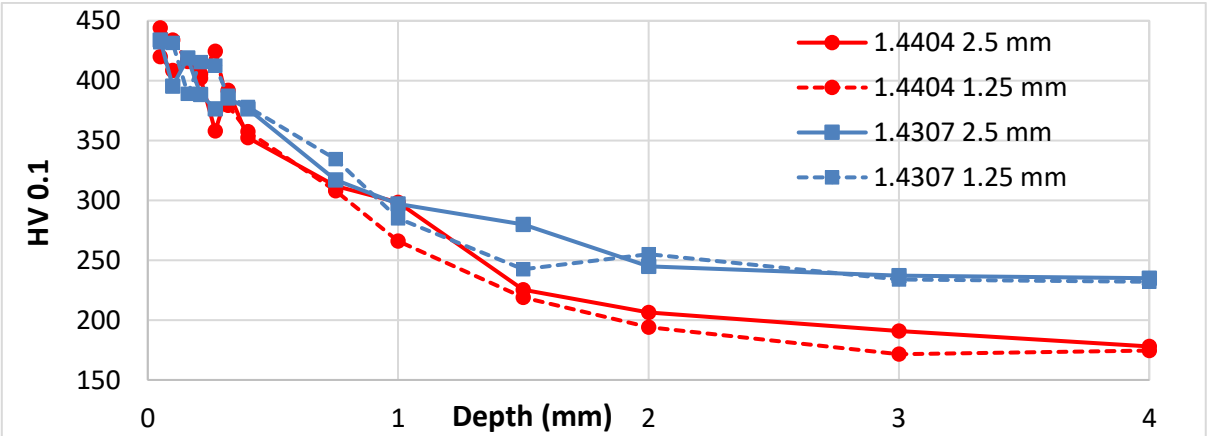

Figure 13: Result of the hardness measurements (HV 0.1) on both materials in two notches per sample. The hardness values are connected to achieve better visualisation of the results.

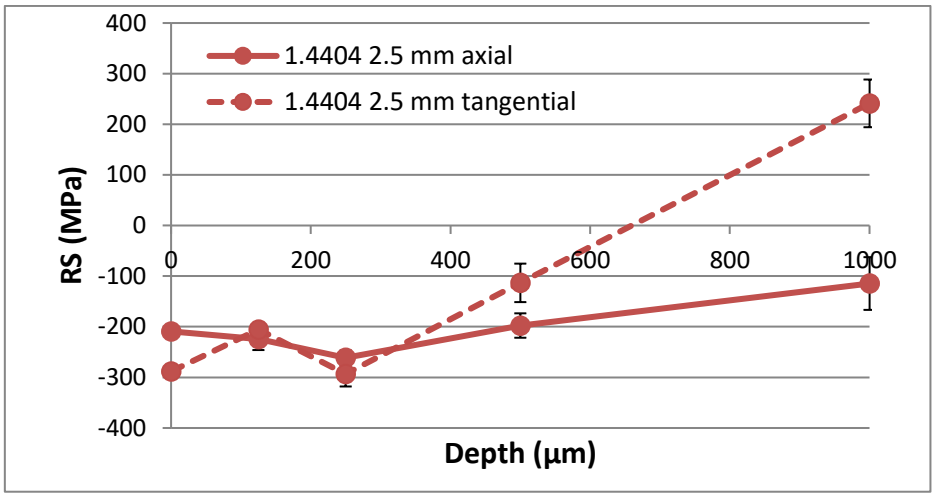

Figure 14: Depth profile of the residual stresses in austenite for 1.4404

Acknowledgements

The authors acknowledge the funding by the Deutsche Forschungsgemeinschaft (DFG, German Research Foundation) - OE 558/16-1, GR1818/63-1.

Literature

[1] Rauschnabel E, Schmidt V. Modern applications of radial forging and swaging in the automotive industry. Journal of Materials Processing Technology 1992; 35: 371–383

[2] DIN 8583-5:2003-09: Manufacturing processes forming under compressive conditions.

[3] Groche P, Fritsche D, Tekkaya EA et al. Incremental Bulk Metal Forming. CIRP annals 56.2007, No.2, p. 635-656; DOI: 10.1016/j.cirp.2007.10.006

[4] Ishkina S, Charni D, Herrmann M et al. Influence of Process Fluctuations on Residual Stress Evolution in Rotary Swaging of Steel Tubes. Materials, 2019, 12, 6, p. 855ff; DOI: 10.3390/ma12060855

[5] Charni D, Ishkina S, Epp J et al. Generation of residual stresses in rotary swaging process. MATEC Web Conferences 2018, 190, 04001; DOI: 10.1051/matecconf/201819004001

[6] Biehler J, Hoche H, Oechsner M, Kaestner P, Bunk K. Bräuer G. Influence of the microstructure on the corrosion resistance of plasma-nitrided austenitic stainless steel 304L and 316L, Mat Sci Eng. Tech. 2014, 45, 10, p. 930-946, DOI: 10.1002/mawe.201400329

[7] Hoche H, Balser A, Oechsner M et al. Enhancement of the residual stresses of cold full-forward extruded parts by application of an active counter punch. Mat Sci Eng. Tech. 2019, 50, 6, p. 669-681; DOI: 10.1002/mawe.201900050

[8] Spieß L, Teichert G, Schwarzer R, Behnken H, Genzel C. Moderne Röntgenbeugung: Röntgendiffrak-tometrie für Materialwissenschaftler, Physiker und Chemiker. 2 Aufl. Wiesbaden, Cham: Vie-weg+Teubner Verlag; Springer International Publishing AG; 2009

[9] Eigenmann B, Macherauch E. Röntgenographische Untersuchung von Spannungszuständen in Werkstoffen. Teil II. Fortsetzung von Matwiss. und Werktoffechn. 3, 1995, p. 148-160; DOI: 10.1002/mawe.19950260410